Extending the global gradient algorithm to unsteady flow extended period simulations of water distribution systems

Ezio Todini

ABSTRACT

This paper introduces an extension of the Global Gradient Algorithm (GGA) to directly solve unsteady flow problems arising from the presence of variable head water storage devices, such as tanks, in Extended Period Simulations (EPS) of looped water distribution networks (WDN). Such a modification of the original algorithm was motivated by the need to overcome oscillations and instabilities reported by several users of EPANET, a worldwide available package, which uses the GGA to solve the looped WDN equations. The set of partial differential equations describing the time and space behaviour of a water distribution system is here presented. It is shown how an unsteady flow GGA can be derived by simple modifications of the original steady-state GGA. The performances of the new algorithm, referred to as EPS-GGA, are compared with the results provided by EPANET on an extremely simplified example, the solution of which is qualitatively known. As opposed to EPANET which shows significant instabilities, the EPS-GGA is stable under a wide variety of increasing integration time intervals.

Key words | extended period simulation, global gradient algorithm, integration of partial differential equations, water distribution networks

Ezio Todini
Dipartimento di Scienze della Terra e Geologico Ambientali,
Università di Bologna,
Via Zamboni 67,
40126 Bologna,
Italy
E-mail: *ezio.todini@unibo.it*

INTRODUCTION

Introduced by Todini (1979) and Todini & Pilati (1988), the Global Gradient Algorithm (GGA) was chosen by Rossman (1993) as the hydraulic algorithm for the development of EPANET, the US Environmental Protection Agency NETwork analysis package, which, in the last decades, has become the standard in Water Distribution Network (WDN) analysis. EPANET has also given rise to a wide variety of commercial packages, e.g. WaterGems (Bentley Systems 2006) and MIKEURBAN (DHI 2008) which make use of the hydraulic EPANET engine for the solution of looped WDNs. In the past decade, GGA was also extended to include direct computation of the speed coefficient of variable speed pumps (Todini *et al.* 2007; Wu *et al.* 2009) as well as pressure-driven demand (Todini 2003; Giustolisi *et al.* 2008*a*,*b*).

The GGA, together with all the other available algorithms e.g. the Nodal Gradient developed by Martin & Peters (1963) and extended to solve for pumps and valves by Shamir & Howard (1968); the Simultaneous Loops developed by Epp & Fowler (1970); and the Linear Theory method developed by Wood & Charles (1972) were basically developed for the solution of the so-called 'network analysis problem'. This type of solution is needed in the classical design problem, which performs a steady-state analysis of the network based on assigned design conditions such as the network topology, the pipes lengths and diameters, the maximum demand, etc. to verify whether the considered pipe diameters are large enough to guarantee water delivery at each demand node with sufficient head under several operating conditions.

For control purposes, users have become more interested in the simulation of the time evolution of flows and pressures in WDNs. Extended Period Simulation (EPS)

doi: 10.2166/hydro.2010.164

capabilities have therefore been introduced (Rao & Bree 1977; Rao *et al.* 1977; Bhave 1988). These allow for the simulation of the slow variation in flow conditions with time, e.g. due to the diurnal changes of demand, by alternating in time a succession of steady-state analyses at fixed times to a succession of mass balance computations in each of the variable head water storages (generally referred to as tanks). This approach is known in the literature as the Euler method (Wood 1980; Rossman 1993; Ulanicka *et al.* 1998).

In practice, an updated water level is estimated in each tank at the end of the time interval by adding or subtracting to the previous time step water volume stored in the tank, the integral in time of the excess flow, which is generally computed as the product of the time interval times the previous time step excess flow at the node. The estimated water level is then considered as a 'known' water level and a new steady-state network analysis is performed for the new time step.

Improved Euler methods have also been proposed using predictor-corrector schemes (Rao & Bree 1977; Rao *et al.* 1977; Bhave 1988; Brdys & Ulanicki 1994; Water Research Centre 1994). More recently, an 'explicit integration method' was also proposed by Van Zyl *et al.* (2006). All these authors decouple the integration in time of the tank mass balance equations from the steady-state network solutions at fixed time (also called 'snapshots').

If the variable storage devices are not present in the network, or if they are relatively far away, all these approaches seem to correctly perform. However, several users of EPANET (as well as of the commercial packages that use EPANET as the hydraulic engine) have reported anomalous oscillations of the water level of two (or more) tanks, particularly when the distance and the friction losses of the pipes connecting them are relatively small.

The purpose of this paper is therefore to provide a solution to this problem by showing how an unsteady formulation of the GGA can lead to unconditionally stable WDN simulations.

THE UNSTEADY FLOW FORMULATION

In Extended Period Simulation of Water Distribution Networks, slow time-varying conditions in the network (such as changes in the demand, changes in water storage accumulation, etc.) have to be taken into account. These changes generally induce relatively slow unsteady flow conditions with negligible inertial and dynamical effects, as opposed to what happens in the presence of waterhammer phenomena.

Therefore, in the absence of important inertial and dynamical effects, the unsteady flow problem in WDNs can be reduced to the following mass and momentum balance equations:

$$\begin{cases} \dfrac{\partial V_i}{\partial t} = \displaystyle\sum_k^{n_i} Q_{ik} + q_i \\ \dfrac{\partial h}{\partial x} = -K|Q|^{n-1}Q \end{cases} \tag{1}$$

where V_i is the volume of water stored in node i; Q_{ik} is the flow in the pipe connecting nodes i and k; q_i is the external inflow to node i (which implies that user's demand wil be negative); n_i is the number of nodes connected to node i; h is the water head; K is the resistance coefficient which depends on the chosen expression describing the head losses; n is the exponent of the chosen head losses formula; t is the time coordinate and x is the space coordinate taken along the generic pipe.

The first set of equations describes the mass balance at each of the unknown head nodes (including tanks which are considered here as unknown head nodes) and the second set describes the losses along each pipe. Please note that Equation (1) has been written as a set of partial differential equations since it is derived from a simplification of the more general equations by disregarding the local and the convective acceleration terms. This is why Equation (1) cannot be used to study fast transients such as waterhammer oscillations (where the reproduction of the inertial effects becomes essential) but is deemed sufficient to reproduce the relatively slow variation in flow conditions with time due to change in the boundary conditions due to demand and the slow opening and closing of valves.

The problem with EPANET and with most of the presently available approaches is the fact that, given the absence of cross terms such as the space derivative of head in the mass balance equations and time derivative of volume in the momentum equation, they integrate the mass balance equations in time separately from the integration in space of

the momentum equations. In practice, without explicitly stating it, they solve the following two ordinary differential equation problems. The first is the integration in space at fixed time (the so-called snapshot):

$$\begin{cases} \sum_{k}^{n_i} Q_{ik} + q_i = 0 \\ \dfrac{dh}{dx} = -K|Q|^{n-1}Q \end{cases} \tag{2}$$

while the second is the integration in time of the mass balance equation. This is carried out at specific locations (the tanks) independently of any spatial interaction by using classical schemes such as the Euler, the Runge-Kutta or the Milne predictor-corrector:

$$\frac{dV_i}{dt} = \sum_{k}^{n_i} Q_{ik} + q_i \tag{3}$$

As can be noted from Equations (2) and (3), the partial derivatives have been substituted by the substantial derivatives and the two sets of equations are integrated independently of one another.

When the classical steady-state formulation applies, e.g. when the time variation of storage is null (which is true for all the nodes apart from the tanks), Equation (2) is sufficient to describe the WDN behaviour. However, the de-coupled use of Equation (3) is incorrect when dealing with the more general problem in which variable storage devices are included. In numerical analysis it is well known that Euler or more sophisticated schemes, such as Runge-Kutta or Milne, can only be used to solve systems of ordinary differential equations and cannot be applied to partial differential equations. Decoupling the original equations to integrate them as two different systems of ordinary differential equations inevitably leads to the loss of the cross space-time interactions represented by Equation (1).

It is evident that space and time integration must be carried out at the same time to avoid losing the coherence in the spatial and temporal behaviour. Any variation in time at a node will inevitably influence the surrounding nodes at a celerity, which characterizes the phenomenon. When two or more tank storage nodes are not far apart, this interaction becomes substantial and, if not accounted for, instabilities in the form of oscillations will be generated as a means to compensate the integration errors.

Unfortunately this problem has received scant attention in the past decade. Only Filion & Karney (2000) tried to introduce the unsteady flow effects via a separated transient simulator (a waterhammer model), which analyses a short time transient at the beginning and at the end of a time-step and then uses the acquired information in a modified improved Euler scheme. Apart from the fact that in practice they still separate the integration in time from the integration in space, the improvements they obtained were inevitably paid for in terms of system information requirements and computational efforts.

One could argue that, although not fully correct, all these approaches (apart from the latter) are quite simple to implement and conveniently allow the use of packages based on algorithms originally developed for steady-state problems (e.g. the WDN analysis problem) to be extended to EPS. On the contrary, this paper demonstrates that a correct solution of the unsteady state problem in WDNs can actually be found by extending the GGA algorithm to solve the unsteady flow problem; that it does not require larger computational efforts than the presently used 'Euler integration in time + snapshot' and, last but not least, that it can be easily incorporated in the currently available packages based on the GGA.

EXTENSION OF THE GGA TO SOLVE THE UNSTEADY FLOW PROBLEM

The extension of the GGA to slow unsteady flow WDNs problems typical of EPS can be derived as follows. The change in storage of a tank can also be represented as a function of the water surface elevation h_i as:

$$\frac{\partial V_i}{\partial t} = \Omega_{i,h_i}\frac{\partial h_i}{\partial t} \quad \forall\, h_i \geq h_{0,i} \tag{4}$$

where Ω_{i,h_i} is the area of the tank in node i, which is a function of the water elevation h_i, while $h_{0,i}$ is the elevation of the tank bottom. If $h_i < h_{0,i}$ the storage derivative of Equation (4) is obviously zero given that $\Omega_{i,h_i} = 0$ when $h_i < h_{0,i}$. Equation (4) can be substituted into the first set of Equation (1) to give:

$$\Omega_i\frac{\partial h_i}{\partial t} = \sum_{k}^{n_i} Q_{ik} + q_i \tag{5}$$

Equation (5) can be discretized in time using an implicit scheme based on the appropriate choice of a time-averaging weight $\vartheta(0 \le \vartheta \le 1)$:

$$\bar{\Omega}_{i,h_{i,t},h_{i,t-\Delta t}} \frac{h_{i,t} - h_{i,t-\Delta t}}{\Delta t} = \vartheta\left(\sum_k^{n_i} Q_{ik,t} + q_{i,t}\right) + (1-\vartheta)\left(\sum_k^{n_i} Q_{ik,t-\Delta t} + q_{i,t-\Delta t}\right) \quad (6)$$

where $\bar{\Omega}_{i,h_{i,t},h_{i,t-\Delta t}}$ is the average tank cross section in the Δt interval, defined as:

$$\bar{\Omega}_{i,h_{i,t},h_{i,t-\Delta t}} = \frac{1}{h_{i,t} - h_{i,t-\Delta t}} \int_{h_{i,t-\Delta t}}^{h_{i,t}} \Omega_{i,h_i} \mathrm{d}h_i \quad (7)$$

in the more general case.

If the water level in the tank drops below the tank bottom, Ω can be set to zero and the tank will correctly behave as a junction without storage accumulation. If the water level overtops the tank, a correction of the water level and the corresponding mass balance has to be made. This will be discussed in the section relevant to the GGA-EPS algorithm derivation.

Please note that in Equation (6) and the following equations, time has been introduced in the form of an index.

Equation (6) can be rewritten as:

$$\sum_k^{n_i} Q_{ik,t} - \frac{\bar{\Omega}_{i,h_{i,t},h_{i,t-\Delta t}}}{\vartheta \Delta t} h_{i,t} = -q_{i,t} - \frac{(1-\vartheta)}{\vartheta}\left(\sum_k^{n_i} Q_{ik,t-\Delta t} + q_{i,t-\Delta t}\right) - \frac{\bar{\Omega}_{i,h_{i,t},h_{i,t-\Delta t}}}{\vartheta \Delta t} h_{i,t-\Delta t} \quad (8)$$

to be appropriately introduced in the GGA formulation. Equation (8) is specific to the 'tank' nodes, since all demand nodes (junctions) are characterized by $\bar{\Omega}_{i,h_{i,t},h_{i,t-\Delta t}} = 0$ and the reservoir nodes (fixed head nodes) by $\mathrm{d}V/\mathrm{d}t = 0$. Therefore, for all the demand nodes the equations to be solved are the same as for the steady-state problem because if

$$\sum_k^{n_i} Q_{ik,t-\Delta t} + q_{i,t-\Delta t} = 0$$

holds at time $t - \Delta t$ it can be immediately verified that $\sum_k^{n_i} Q_{ik,t} + q_{i,t} = 0$ will also hold at time t.

When solving unsteady flow problems, it is common practice to start from a steady state. The initial condition for solving Equation (1) can therefore be found at time $t = 0$ using the presently available snapshot approaches. These solve the system of Equation (2) with tanks considered, similarly to reservoirs, as fixed head nodes.

Note that at any time $t > 0$, the new formulation considers the level of the tank (and not the inflow to the tank) as the unknown in the solution of the GGA. This implies that if at time $t = 0$ the number of unknowns equals the number of junctions, at time $t > 0$ the number of unknowns must equal the number of junctions + the number of tanks. This differs considerably from the approach taken by the currently available packages, where the tank level is computed prior to the GGA new step and then the tank is considered as a fixed head node in the solution. As a consequence, in this new development the nodal demands $q_{t-\Delta t}$ and q_t will also be allowed to differ from zero. As a matter of fact, non-null flows may occur in the case of direct refilling from external sources (inflow to the tank through a tap or using an external pump not connected to the network) or direct spilling from the tank (as in the case of overflows).

Five main differences will be introduced with respect to the currently available hydraulic simulation packages.

1. A system of partial differential equations will be solved in time and space instead of two systems of ordinary differential equations, one in time and one in space.
2. As opposed to the explicit solution on which most of the packages are based, an implicit solution of the equations will be used by the extension of the GGA to unsteady flow problems. Note that the proposed implicit scheme, which uses a slightly modified GGA to include storage time variation at the tank nodes, is equivalent to and requires the same computational effort as the Euler integration in time + snapshot approach. The latter uses the GGA for the solution of the non-linear steady-state problem at the end of each integration time step.
3. While in current practice the integration is only performed locally using the single tank mass balance equation, in the extended GGA the integration of the time derivatives will also take into account their spatial effects.
4. For the tank nodes, the unknown is the water head and not the nodal flow and mass unbalance as in the currently available packages.

5. For the tank nodes, one can additionally specify external spills or direct refilling from external sources.

In order to simplify the derivation of the EPS-GGA, the dependence of $\bar{\Omega}_{i,h_{i,t},h_{i,t-\Delta t}}$ on $h_{i,t}$ will be taken into account in the estimation of $\bar{\Omega}_{i,h_{i,t},h_{i,t-\Delta t}}$. However, it will be disregarded for the time being without loss of generality in the differentiation of the equations when applying the Newton–Raphson algorithm. This dependence, if needed for improving the convergence, may be introduced in further developments.

Following the formulation of the GGA given in Todini & Pilati (1988), the unsteady flow problem in looped WDNs can be formulated as follows:

$$\begin{bmatrix} \boldsymbol{A}_{11}^t & \vdots & \boldsymbol{A}_{12} \\ \cdots & \cdots & \cdots \\ \boldsymbol{A}_{21} & \vdots & \boldsymbol{A}_{22}^t \end{bmatrix} \begin{bmatrix} \boldsymbol{Q}_t \\ \cdots \\ \boldsymbol{H}_t \end{bmatrix} = \begin{bmatrix} -\boldsymbol{A}_{10}\boldsymbol{H}_{0,t} \\ \cdots \\ -\boldsymbol{q}_t^* \end{bmatrix} \tag{9}$$

The difference from the original GGA lies in the introduction of the time coordinate, the presence of a non-null diagonal matrix $\boldsymbol{A}_{22}^t$ and a differently defined vector $\boldsymbol{q}_t^*$. The quantities appearing in Equation (9) are defined as:

$$\boldsymbol{Q}_t^{\boldsymbol{T}} = [Q_{1,t}, Q_{2,t}, \cdots, Q_{n_p,t}]$$

: the $[1, n_p]$ unknown pipe discharges;

$$\boldsymbol{H}_t^{\boldsymbol{T}} = [h_{1,t}, h_{2,t}, \cdots, h_{n_n,t}]$$ the $[1, n_n]$ unknown nodal heads;

$$\boldsymbol{H}_{0,t}^{\boldsymbol{T}} = [h_{n_n+1,t}, h_{n_n+2,t}, \cdots, h_{n_t,t}]$$

: the $[1, n_{\text{tot}} - n_n]$ known nodal heads; and

$$\boldsymbol{q}_t^{*\boldsymbol{T}} = [q_{1,t}, q_{2,t}, \cdots, q_{n_n,t}]$$: the $[1, n_n]$ known nodal demands,

appropriately modified as described in the following for the tank nodes;

where n_p is the number of pipes; n_n is the number of unknown head nodes; n_{tot} is the total number of nodes in the network; and $n_{\text{tot}} - n_n$ is the number of nodes with known head.

In Equation (9), $\boldsymbol{A}_{11}^t$ is a diagonal matrix. Its elements, including minor losses, are defined for $k \in 1, n_p$; $i \in 1, n_{\text{tot}}$; $j \in 1, n_{\text{tot}}$ where k is the index of the pipe connecting nodes i,j. Note that in the following, index k will be used to identify the position of the element in the matrices, while the symbol ij will be used to identify the relevant pipe:

$$\boldsymbol{A}_{11}^t(k,k) = r|Q_{ij,t}|^{n-1} + m|Q_{ij,t}| \tag{10}$$

for pipes and:

$$\boldsymbol{A}_{11}^t(k,k) = -\frac{\omega^2(h_0 - r(Q_{ij,t}/\omega)^n)}{Q_{ij,t}} \quad \text{or}$$
$$\boldsymbol{A}_{11}^t(k,k) = -\left(\frac{a_0\omega^2}{Q_{ij,t} + b_0\omega + c_0 Q_{ij,t}}\right) \tag{11}$$

(or other similar equations) for pumps.

In Equations (10) and (11), r is the losses coefficient, m is the minor losses coefficient, n is an exponent, ω is the variable speed pumps coefficient, and a_0, b_0 and c_0 are three coefficients of the quadratic function representing the pump characteristic curve. Note that in reality all the coefficients r, m, n, ω, a_0, b_0, c_0 are relevant to specific pipes or pumps; the ij indexes have been omitted to more closely follow the representation given in EPANET.

Matrix $\boldsymbol{A}_{22}^t$ is a $[n_n, n_n]$ diagonal matrix whose generic element is defined as:

$$\boldsymbol{A}_{22}^t(i,i) = 0 \tag{12}$$

for the junction nodes and

$$\boldsymbol{A}_{22}^t(i,i) = -\frac{\bar{\Omega}_{i,h_{i,t},h_{i,t-\Delta t}}}{\vartheta \Delta t} \tag{13}$$

for all the variable head water storage nodes (tanks).

The quantity $\boldsymbol{q}_t^*$ on the right-hand side can be defined as:

$$\boldsymbol{q}_t^*(i) = q_{i,t} \tag{14}$$

for the junction nodes and

$$\boldsymbol{q}_t^*(i) = q_{i,t} + \frac{(1-\vartheta)}{\vartheta}\left(\sum_k^{n_i} Q_{ik,t-\Delta t} + q_{i,t-\Delta t}\right) + \frac{\bar{\Omega}_{i,h_{i,t},h_{i,t-\Delta t}}}{\vartheta \Delta t} h_{i,t-\Delta t} \tag{15}$$

for all the variable head water storage nodes (tanks).

These equations can also be written in matrix form as:

$$\boldsymbol{q}_t^* = \boldsymbol{q}_t \tag{14a}$$

for the junction nodes and

$$\boldsymbol{q}_t^* = \boldsymbol{q}_t + \frac{1-\vartheta}{\vartheta}(\boldsymbol{A}_{21}\boldsymbol{Q}_{t-\Delta t} + \boldsymbol{q}_{t-\Delta t}) - \boldsymbol{A}_{22}^{t-\Delta t}\boldsymbol{H}_{t-\Delta t} \tag{15a}$$

for all the variable head water storage nodes (tanks).

The actual network topology is then described by means of a topological incidence matrix $\bar{\boldsymbol{A}}_{12}$ defined as follows, with the convention that inflows to a node are assumed positive and outflows negative:

$$\bar{\boldsymbol{A}}_{12}(i,j) = \begin{cases} -1 & \text{if the flow of pipe } j \text{ leaves node } i \\ 0 & \text{if pipe } j \text{ is not connected to node } i \\ +1 & \text{if the flow of pipe } j \text{ enters node } i \end{cases} \tag{16}$$

The uniqueness of the solution of Equation (9) requires at least one node with known head. The overall incidence matrix, which is an $[n_p,\ n_{\text{tot}}]$ matrix, can thus be partitioned into the two matrices:

$$\bar{\boldsymbol{A}}_{12} = [\boldsymbol{A}_{12} \vdots \boldsymbol{A}_{10}] \tag{17}$$

relating the pipes to the nodes with unknown head ($\boldsymbol{A}_{12}$) and to the nodes with known head ($\boldsymbol{A}_{10}$). For the sake of clarity, the notation $\boldsymbol{A}_{10} = \boldsymbol{A}_{01}^{\boldsymbol{T}}$ and $\boldsymbol{A}_{12} = \boldsymbol{A}_{21}^{\boldsymbol{T}}$ is used.

Following the original derivation by Todini & Pilati (1988), the Newton–Raphson technique is applied for the solution of the system of the linear and non-linear Equation (9), which can be re-written as:

$$\begin{bmatrix} \boldsymbol{A}_{11}^t & \vdots & \boldsymbol{A}_{12} \\ \cdots & \cdots & \cdots \\ \boldsymbol{A}_{21} & \vdots & \boldsymbol{A}_{22}^t \end{bmatrix} \begin{bmatrix} \boldsymbol{Q}_t \\ \cdots \\ \boldsymbol{H}_t \end{bmatrix} + \begin{bmatrix} \boldsymbol{A}_{10}\boldsymbol{H}_{0,t} \\ \cdots \\ \boldsymbol{q}_t^* \end{bmatrix} = \begin{bmatrix} 0 \\ \cdots \\ 0 \end{bmatrix} \tag{18}$$

If only an approximate solution $\boldsymbol{Q}_t^0$, $\boldsymbol{H}_t^0$ is known, the right-hand side of Equation (18) will not be null. Equation (18) can therefore be written as:

$$\begin{bmatrix} \boldsymbol{A}_{11}^t & \vdots & \boldsymbol{A}_{12} \\ \cdots & \cdots & \cdots \\ \boldsymbol{A}_{21} & \vdots & \boldsymbol{A}_{22}^t \end{bmatrix} \begin{bmatrix} \boldsymbol{Q}_t^0 \\ \cdots \\ \boldsymbol{H}_t^0 \end{bmatrix} + \begin{bmatrix} \boldsymbol{A}_{10}\boldsymbol{H}_{0,t} \\ \cdots \\ \boldsymbol{q}_t^* \end{bmatrix} = \begin{bmatrix} \boldsymbol{E}1 \\ \cdots \\ \boldsymbol{E}2 \end{bmatrix} \tag{19}$$

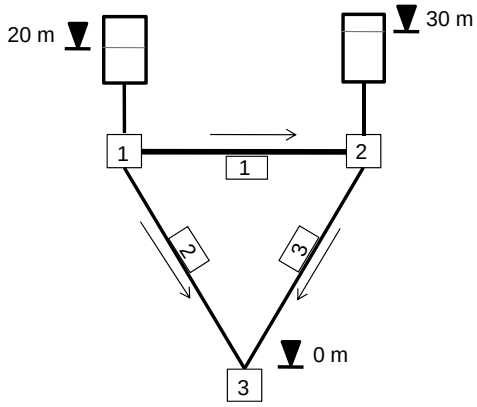

Figure 1 | Schematic representation of the first example. Two emptying interconnected tanks starting at time zero with different water levels.

Recalling that $\boldsymbol{A}_{11}^t$ is also a function of the approximate solution, by differentiating Equation (19) with respect to the unknowns, we obtain:

$$\begin{bmatrix} \boldsymbol{D}_{11}^t & \vdots & \boldsymbol{A}_{12} \\ \cdots & \cdots & \cdots \\ \boldsymbol{A}_{21} & \vdots & \boldsymbol{A}_{22}^t \end{bmatrix} \begin{bmatrix} \mathrm{d}\boldsymbol{Q}_t \\ \cdots \\ \mathrm{d}\boldsymbol{H}_t \end{bmatrix} = \begin{bmatrix} \mathrm{d}\boldsymbol{E}1 \\ \cdots \\ \mathrm{d}\boldsymbol{E}2 \end{bmatrix} \tag{20}$$

where $\boldsymbol{D}_{11}^t$ is a $[n_p, n_p]$ diagonal matrix, n_{tot}, with elements defined for $k \in 1, n_p$; $i \in 1, n_{\text{tot}}$; $j \in 1, n_t$ as:

$$\boldsymbol{D}_{11}^t(k,k) = nr|Q_{ij,t}|^{n-1} + 2m|Q_{ij,t}| \tag{21}$$

for pipes and:

$$\boldsymbol{D}_{11}^t(k,k) = nr\omega^{2-n}|Q_{ij,t}|^{n-1} \quad \text{or} \qquad \boldsymbol{D}_{11}^t(k,k) = -(b_0\omega + 2c_0Q_{ij,t}) \tag{22}$$

for pumps according to the chosen model.

Table 1 | Pipe characteristics

Pipe number	Head node	Tail node	Length (m)	Diameter (mm)	Hazen–Williams roughness coefficient	Minor loss coefficient
1	1	2	100	200	130	0
2	1	3	100	100	130	0
3	2	3	100	100	130	0

Table 2 | Junctions operating parameters (tanks)

Junction number	Initial head (m)	Diameter (m)
1	20.00	3.56
2	30.00	3.56

Table 3 | Junctions operating parameters (fixed head nodes)

Junction number	Head (m)
3	0.0

Matrix $\boldsymbol{D}_{22}^t$ is a $[n_n, n_n]$ diagonal matrix whose generic element is defined as:

$$\boldsymbol{D}_{22}^t(i,i) = 0 \tag{23}$$

for all the junction nodes, and

$$\boldsymbol{D}_{22}^t = -\frac{\bar{\Omega}_{i,h_{i,t},h_{i,t-\Delta t}}}{\vartheta \Delta t} \tag{24}$$

for all the tank nodes.

Equation (20) can be discretized assuming a local linearization between the solution at iteration τ and at iteration $\tau+1$, by defining:

$$\begin{aligned} \mathrm{d}\boldsymbol{Q}_t &= \boldsymbol{Q}_t^{\tau} - \boldsymbol{Q}_t^{\tau+1} \\ \mathrm{d}\boldsymbol{H}_t &= \boldsymbol{H}_t^{\tau} - \boldsymbol{H}_t^{\tau+1} \\ \mathrm{d}\boldsymbol{E}1_t &= \boldsymbol{A}_{11}\boldsymbol{Q}_t^{\tau} + \boldsymbol{A}_{12}\boldsymbol{H}_t^{\tau} + \boldsymbol{A}_{10}\boldsymbol{H}_{0,t}^{\tau} \\ \mathrm{d}\boldsymbol{E}2_t &= \boldsymbol{A}_{21}\boldsymbol{Q}_t^{\tau} + \boldsymbol{A}_{22}\boldsymbol{H}_t^{\tau} + \boldsymbol{q}_t^{*} \end{aligned} \tag{25}$$

Substituting Equation (25) into Equation (20) and analytically solving the system of equations, the iterative formulation of the EPS-GGA algorithm is:

$$\begin{cases} \boldsymbol{H}_t^{\tau+1} = \boldsymbol{A}_t^{-1}\boldsymbol{F}_t \\ \boldsymbol{Q}_t^{\tau+1} = \boldsymbol{Q}_t^{\tau} - \left(\boldsymbol{D}_{11}^t\right)^{-1}\left(\boldsymbol{A}_{11}^t\boldsymbol{Q}_t^{\tau} + \boldsymbol{A}_{12}\boldsymbol{H}_t^{\tau+1} + \boldsymbol{A}_{10}\boldsymbol{H}_{0,t}\right) \end{cases} \tag{26}$$

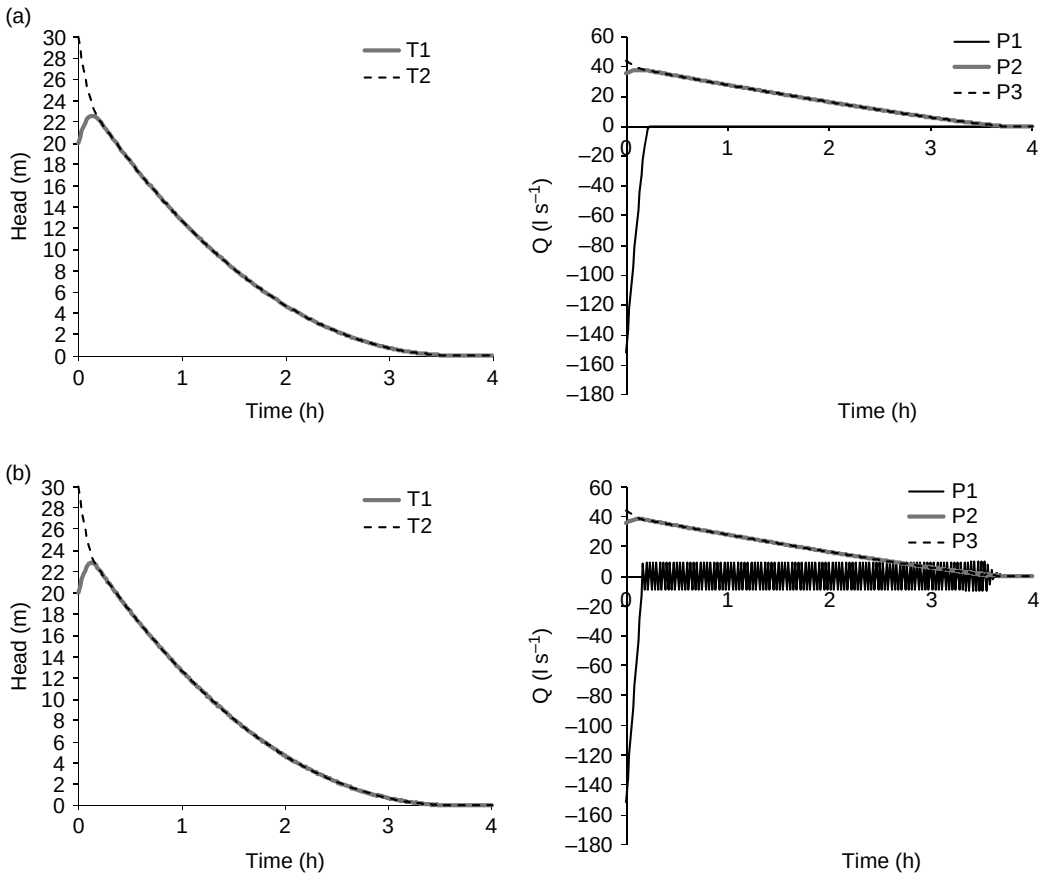

Figure 2 | (a) Results obtained using the EPS-GGA approach with integration time step $\Delta t = 1$ min. Note the absence of instability in the flow of Pipe 1 and in the tanks water level. (b) Results obtained using the EPANET 2 with integration time step $\Delta t = 1$ min. Note the marked oscillations in the flow of pipe 1 even at this short integration time step.

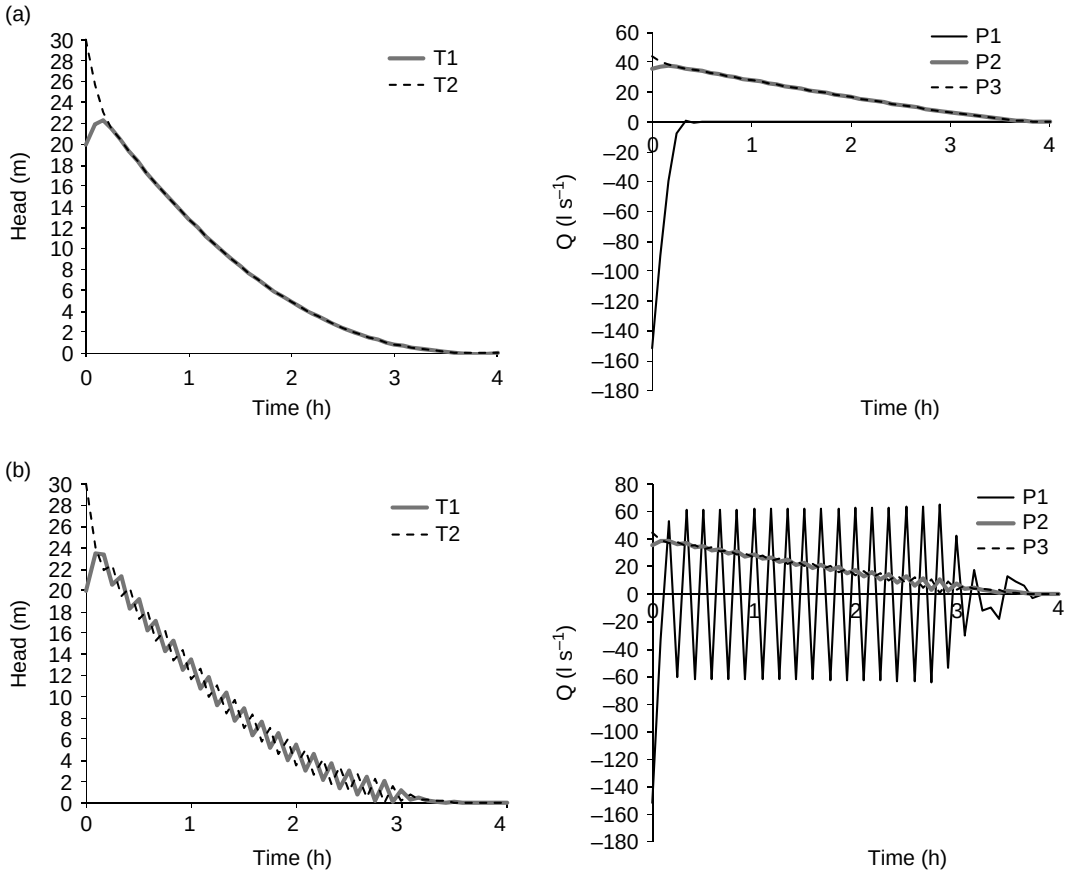

Figure 3 | As for Figure 2 with $\Delta t = 5$ min. Note the marked oscillations in the flow of pipe 1 together with the appearance of water level oscillations in both tanks.

where

$$\boldsymbol{A}_t = \boldsymbol{A}_{21}(\boldsymbol{D}_{11}^t)^{-1}\boldsymbol{A}_{12} - \boldsymbol{D}_{22}^t \tag{27}$$

and

$$\boldsymbol{F}_t = \boldsymbol{A}_{21}\boldsymbol{Q}_t^\tau + \boldsymbol{A}_{22}\boldsymbol{H}_t^\tau - \boldsymbol{A}_{21}(\boldsymbol{D}_{11}^t)^{-1}\boldsymbol{A}_{11}^t\boldsymbol{Q}_t^\tau - \boldsymbol{A}_{21}(\boldsymbol{D}_{11}^t)^{-1}\boldsymbol{A}_{10}\boldsymbol{H}_{0,t} + \boldsymbol{q}_t^* \tag{28}$$

As can be noted, the problem is reduced to the iterated solution of a symmetrical and sparse matrix of size $[n_n, n_n]$ similarly to the original GGA. The only difference from the original GGA, apart from the time index, lies in the presence of the new diagonal matrix $\boldsymbol{D}_{22}^t$ and in the different definition of vector $\boldsymbol{q}_t^*$.

A scalar formulation of this algorithm can also be provided by defining the following quantities in accordance with the notation used by Rossman (1993) in the development of EPANET, namely

$$p_{ij,t} = \frac{1}{nr|Q_{ij,t}^\tau|^{n-1} + 2m|Q_{ij,t}^\tau|} \quad \text{and} \quad y_{ij,t} = p_{ij,t}\left(r\left|Q_{ij,t}^\tau\right|^{n-1} + m\left|Q_{ij,t}^\tau\right|\right) \tag{29}$$

for pipes and:

$$p_{ij,t} = \frac{1}{nr\omega^{2-n}\left|Q_{ij,t}^\tau\right|^{n-1}} \quad \text{and} \quad y_{ij,t} = \frac{-p_{ij,t}\omega^2\left(h_0 - r\left(Q_{ij,t}^\tau/\omega\right)^n\right)}{Q_{ij,t}^\tau} \tag{30}$$

or

$$p_{ij,t} = -\frac{1}{b_0\omega + 2c_0Q_{ij,t}^\tau} \quad \text{and} \quad y_{ij,t} = -p_{ij}\left(a_0\omega^2/Q_{ij,t}^\tau + b_0\omega + c_0Q_{ij,t}^\tau\right) \tag{31}$$

for pumps, according to the chosen model given by Equation (11).

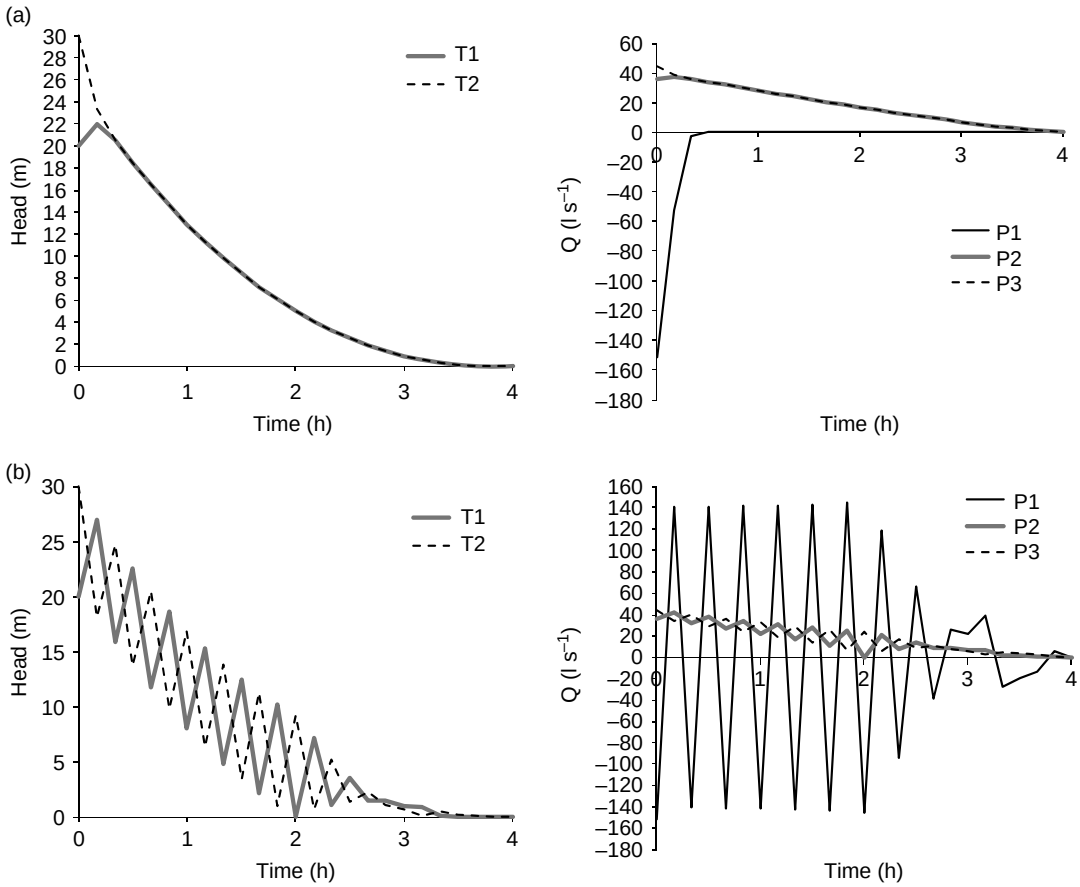

Figure 4 | As for Figure 2 with $\Delta t = 10$ min. Note the marked oscillations in the flow of pipe 1 together with large water level oscillations in both tanks.

Note that in order to avoid problems with the sign a slightly different definition of $y_{ij,t}$ is used in this paper, namely:

$$y_{ij,t} = \frac{\hat{y}_{ij,t}}{Q^{\tau}_{ij,t}} \tag{32}$$

where $\hat{y}_{ij,t}$ is the expression defined in EPANET manual.

In order to introduce the time variant problem in EPANET, it is convenient to define a new variable $\eta_{i,t}$ as:

$$\eta_{i,t} = \boldsymbol{D}^{t}_{22}(i,i) \tag{33}$$

With the given notation, it is therefore possible to define the matrix $\boldsymbol{A}_t$ and vector $\boldsymbol{F}_t$ as follows:

$$\boldsymbol{A}_t(i,i) = \sum_j p_{ij,t} - \eta_{i,t} \quad \forall\, i \cap j \neq \varnothing,\ i \in 1, n_n,\ j \in 1, n_{\text{tot}} \tag{34}$$

$$\boldsymbol{A}_t(i,j) = -p_{ij,t} \quad \forall\, i \cap j \neq \varnothing,\ i,j \in 1, n_n \tag{35}$$

$$\boldsymbol{F}_t(i) = \sum_j (1 - y_{ij,t}) Q^{\tau}_{ij,t} + \sum_f p_{if,t} h^{\tau}_{f,t} + q^{*}_{i,t} \quad \forall \begin{cases} i \in 1, n_n \\ i \cap j \neq \varnothing,\ j \in 1, n_{\text{tot}} \\ i \cap f \neq \varnothing,\ f \in n_n + 1, n_{\text{tot}} \end{cases} \tag{36}$$

The solution of Equation (9) is thus obtainable by repeated iterations of Equation (26) until a sufficient degree of accuracy is reached.

In case the estimated water level is lower than the bottom or if it overtops the upper edge of the tank, the following simple procedure can be used. After updating the head at the junctions and the tank nodes using the first of Equation (26), the resulting water elevation is compared to the bottom level h_0 as well as to the top edge $h_{\max}$ of the tank. If the resulting level is lower than h_0, it is only necessary to set the tank section Ω to zero and the node will behave as a regular junction node. If the resulting water level is higher than $h_{\max}$,

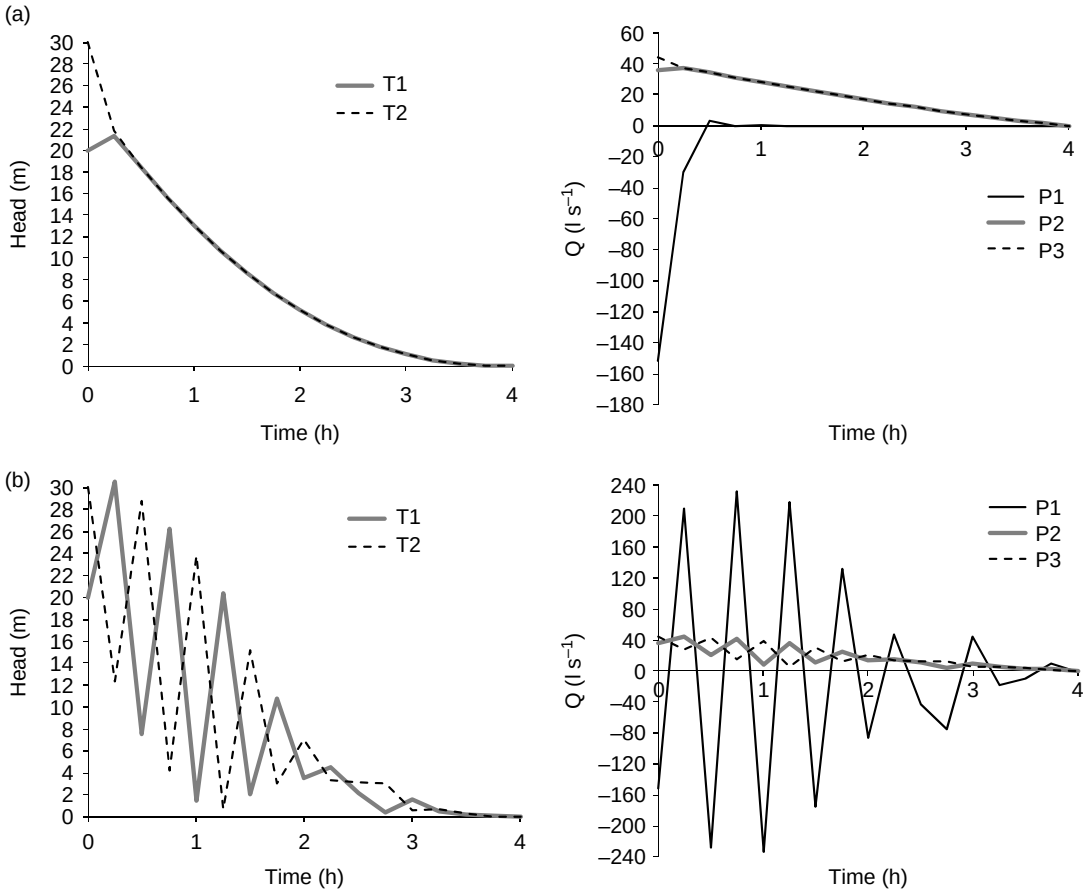

Figure 5 | As for Figure 2 with $\Delta t = 15$ min. Note (a) only a minor instability in the flow of Pipe 1 while the tanks water level is still very stable and (b) the extremely large oscillations in the flow of pipe 1 together with extremely large water level oscillations in both tanks.

the tank node is turned into a fixed head node with $h = h_{\max}$ which will allow the spill from the tank to be computed.

EXAMPLE OF APPLICATION

The following extremely simplified example will be used to illustrate the performance of the new EPS-GGA. The two interconnected tanks with constant cross-section (shown in Figure 1) are emptying. All demands are equal to zero, and the unknowns of the problem are the water level in the two tanks and the flow exiting node 3 (a fixed head node) together with the flow in the three pipes. Pipe characteristics are summarised in Table 1, while Tables 2 and 3 provide the characteristic parameters of the tanks and fixed head nodes used in the example.

Qualitatively, the solution to the problem is known. It is expected that initially a flow from Tank 2 (with water level initially set at 30 m) to Tank 1 (with water level initially set at 20 m) will occur in Pipe 1 until the two tanks reach the same water level. At this point, the flow in Pipe 1 will stop and both the tanks will empty at the same rate.

The Hazen–Williams equation has been used to represent the head losses, which are expressed as:

$$r = \frac{10.67L}{C^{1.852}D^{4.871}} \tag{37}$$

In the case of the example, at time $t = 0$ the steady state is uniquely determined by the initial level in the tanks also taken as fixed head nodes, which gives:

$$\Delta h_{1,2} = h_1 - h_2 = -10 \quad Q_{1,2} = -151.51$$
$$\Delta h_{1,3} = h_1 - h_3 = 20 \quad Q_{1,3} = 35.58$$
$$\Delta h_{2,3} = h_2 - h_3 = 30 \quad Q_{2,3} = 44.29$$

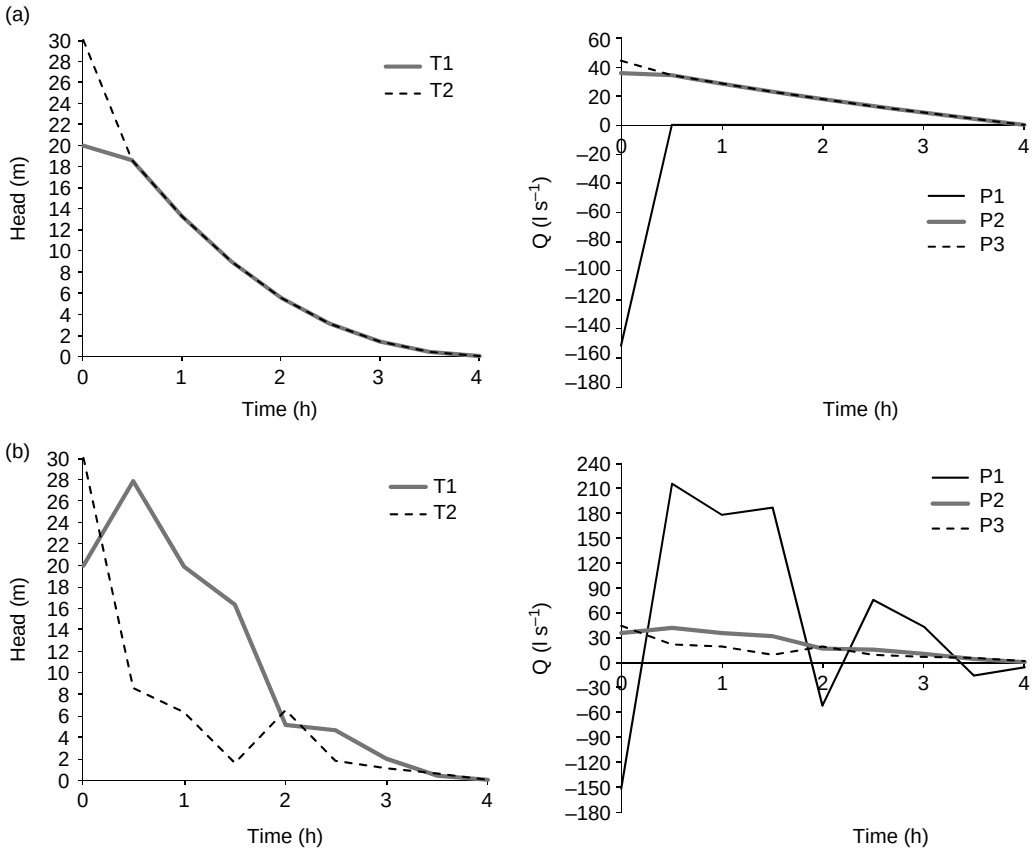

Figure 6 | As for Figure 2 with $\Delta t = 30$ min. (a) the disappearance of the surge in tank 1 is due to the coarse time discretization. (b) Note the large errors in the flow of pipe 1 and in the water level oscillations of both tanks.

At any successive time ($t > 0$) following the newly developed EPS-GGA algorithm, while node 3 is still kept to its fixed head ($h_3 = 0$), the head in the two tanks is considered unknown and the problem can be solved by estimating the quantities:

$$\boldsymbol{A}_t = \begin{bmatrix} p_{1,t} + p_{2,t} - \eta_{1,t} & -p_{1,t} \\ -p_{1,t} & p_{1,t} + p_{3,t} - \eta_{2,t} \end{bmatrix} \tag{38}$$

$$\boldsymbol{F}_t = \begin{bmatrix} -(1-y_{1,t})Q^{\tau}_{1,t} - (1-y_{2,t})Q^{\tau}_{2,t} + p_{2,t}h^{\tau}_{3,t} + \frac{\Omega_{1,h_{1,t-\Delta t}}}{\vartheta \Delta t} h_{1,t-\Delta t} \\ + \frac{1-\vartheta}{\vartheta}(-Q_{1,t-\Delta t} - Q_{2,t-\Delta t}) \\ (1-y_{1,t})Q^{\tau}_{1,t} - (1-y_{3,t})Q^{\tau}_{3,t} + p_{3,t}h^{\tau}_{3,t} \\ + \frac{\Omega_{2,h_{2,t-\Delta t}}}{\vartheta \Delta t} h_{2,t-\Delta t} + \frac{1-\vartheta}{\vartheta}(Q_{1,t-\Delta t} - Q_{3,t-\Delta t}) \end{bmatrix} \tag{39}$$

which are used in the recursive equations:

$$\boldsymbol{H}^{\tau+1}_t = \boldsymbol{A}^{-1}_t \boldsymbol{F}_t \tag{40}$$

$$\boldsymbol{Q}^{\tau+1}_t = \begin{bmatrix} (1-y_{1,t})Q^{\tau}_{1,t} + p_{1,t}(h^{\tau+1}_{1,t} - h^{\tau+1}_{2,t}) \\ (1-y_{2,t})Q^{\tau}_{2,t} + p_{2,t}(h^{\tau+1}_{1,t} - h^{\tau+1}_{3,t}) \\ (1-y_{3,t})Q^{\tau}_{3,t} + p_{3,t}(h^{\tau+1}_{2,t} - h^{\tau+1}_{3,t}) \end{bmatrix} \tag{41}$$

RESULTS AND DISCUSSION

Six different time discretization intervals have been used for the integration in time, namely 1 min, 5 min, 10 min, 15 min, 30 min and 1 hour. The results of the EPS-GGA have been compared with the EPANET 2 (Rossman 2002) Version 2, Build 2.00.12 results, which were obtained for the same time discretization intervals.

EPS-GGA was run with a time averaging weight in the implicit scheme $\vartheta = 0.822$, which was found to be the most appropriate value. Moreover, in order to run the problem using EPANET 2 which requires at least one junction (without fixed head), a slightly modified problem was set-up

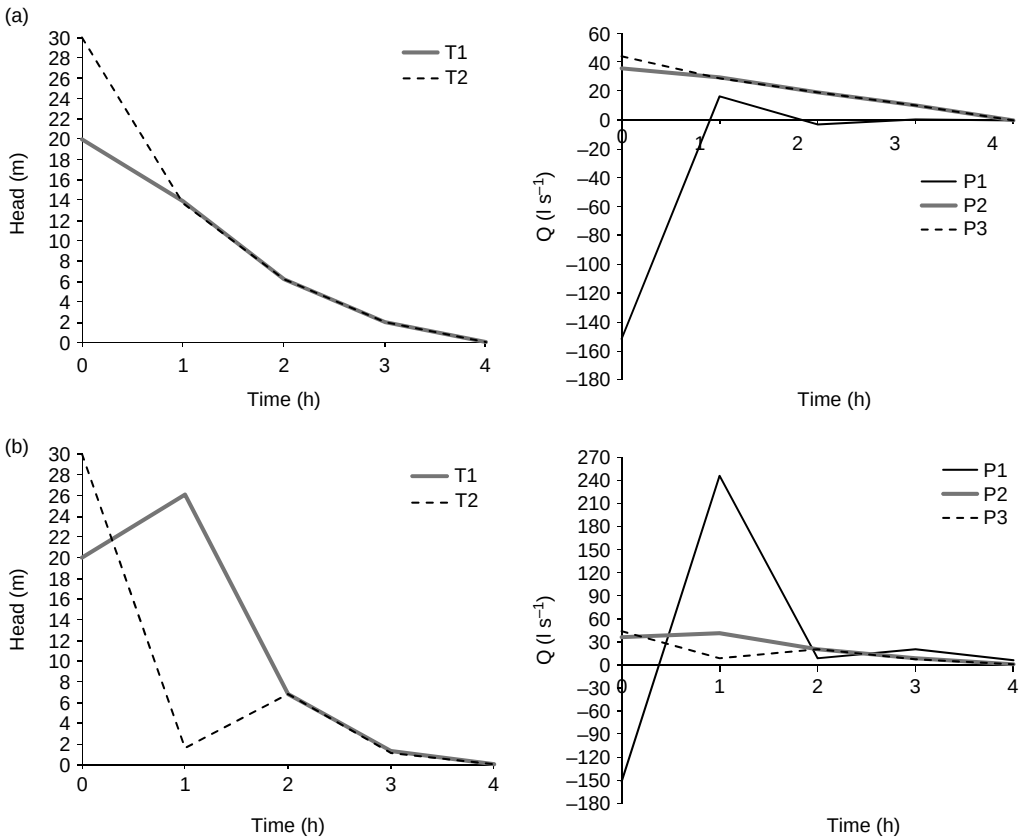

Figure 7 | As for Figure 2 with $\Delta t = 1$ h. (a) Note that the instability in the flow of pipe 1 is caused by the coarse time discretization to compensate the fact that the two tanks reach the same water level after 1 h instead of after approximately 15 min. (b) Note the large errors in the flow of pipe 1 and in the water level oscillations of both tanks.

by adding a null demand junction and a closed pipe connected with Tank n.1, as described in the appendix.

The results obtained with the EPS-GGA are shown in Figures 2(a) (1 min), 3(a) (5 min), 4(a) (10 min), 5(a) (15 min), 6(a) (30 min) and 7(a) (1 h) while the corresponding EPANET 2 results are shown in Figures 2(b) (1 min), 3(b) (5 min), 4(b) (10 min), 5(b) (15 min), 6(b) (30 min) and 7(b) (1 h). In the figures, series T1 and T2 represent the water levels (m) in Tank n.1 and Tank n. 2, while series P1, P2, P3 represent the flow ($l\,s^{-1}$) in pipes n. 1, 2 and 3 respectively.

While the EPS-GGA is practically stable at all time discretization intervals (even when the time step is too coarse to represent the phenomenon), the EPANET 2 is unstable even when the discretization in time is based on 1 min time steps. By increasing the time steps this instability, which initially produces an oscillation in the flow of Pipe 1 connecting the two tanks, is spread to the water levels in the tanks and becomes overwhelming at time steps of 15 min.

CONCLUSIONS

A new extension of the GGA has been presented in this paper, which allows correct representation of unsteady flow in Water Distribution Networks typical of Extended Period Simulations in the presence of a number of variable head storages such as tanks.

It has been clearly demonstrated that the proposed extension of GGA to the EPS-GGA only requires few modifications of the original algorithm and can therefore be easily implemented in the existing computer packages that make use of the GGA as the hydraulic engine (e.g. EPANET and several other commercial packages available in the market). In addition, it requires the same computational effort of the presently used technique known as the 'Euler integration in time + snapshot'.

The EPS-GGA formulation, which integrates the full system of partial differential equations of mass and

momentum balance using an implicit scheme, was tested for the EPANET approach on a simple example with two adjacent tanks. The obtained result not only shows the noticeable improvement of performances of the EPS-GGA with respect to EPANET, but also highlights the extreme stability of the solutions within a wide range of integration time discretization intervals.

It is hoped that the new algorithm will be soon implemented into the EPANET 2 package, since it will require minor changes in the code. It is expected that the relevance of this modification will emerge not only in terms of stability of the hydraulic solutions, but also in terms of its impact on the water-quality problems where the advection-diffusion coefficients can be substantially modified by the oscillatory behaviour of the presently unstable solutions.

ACKNOWLEDGEMENTS

The author would like to acknowledge the stimulating role of Diego Avesani, Paolo Bertola and Maurizio Righetti of the University of Trento, who motivated his interest in studying the reasons for the appearance of water level oscillations of close-by tanks in GGA-based water distribution analysis models.

REFERENCES

Bentley Systems 2006 Incorporated 2006 *WaterGEMS v8 User Manual*. 27 Siemon Co Dr, Suite200W, Watertown, CT06795, USA.

Bhave, P. R. 1988 Extended period simulation of water systems–direct solution. *J. Environ. Eng.* **114** (5), 1146–1159.

Brdys, M. & Ulanicki, B. 1994 *Operational Control of Water Systems: Structures, Algorithms and Applications*. Prentice Hall, London, UK.

DHI, MIKE-URBAN 2008 http://www.dhigroup.com/Software/Urban/MIKEURBAN.aspx

Epp, R. & Fowler, A. G. 1970 Efficient code for steady-state flows in networks. *J. Hydraulics Div.* **96**, Proc. Paper 7002, 43–56.

Filion, Y. R., & Karney, B. W. 2000 Conducting extended period analysis with a transient model. *Proc. 8th Int. Conf. on Pressure Surges*, BHR, Cranfield, UK, pp. 571–585.

Giustolisi, O., Savic, D. A. & Kapelan, Z. 2008*a* Pressure-driven demand and leakage simulation for water distribution networks. *J. Hydraulic Eng.* **134** (5), 626–635.

Giustolisi, O., Kapelan, Z. & Savic, D. A. 2008*b* Extended period simulation analysis considering valve shutdowns. *J. Water Resour. Plann. Manage.* **134** (6), 527–537.

Martin, D. W. & Peters, G. 1963 The application of Newton's method to network analysis by digital computer. *J. Inst. Water Eng.* **17**, 115–129.

Rao, H. S. & Bree, D. W. J. 1977 Extended period simulation of water systems–part A. *J. Hydraulic Div.* **103** (2), 97–108.

Rao, H. S., Markel, L. & Bree, D. J. 1977 Extended period simulation of water systems–part B. *J. Hydraulic Div.* **103** (3), 281–294.

Rossman, L. 1993 *EPANET Users Manual*. EPA-600/R-94/057, Environmental Protection Agency, Risk Reduction Engineering Laboratory, Cincinnati.

Rossman, L. A. 2002 *EPANET 2 Users Manual*. Water Supply and Water Resources Division, National Risk Management Research Laboratory, Cincinnati, OH45268.

Shamir, U. & Howard, C. D. D. 1968 Water distribution systems analysis. *J. Hydraulics Div.* **94**, Proc. Paper 5758, 219–234.

Todini, E. 1979 Un metodo del gradiente per la verifica delle reti idrauliche. *Bollettino degli Ingegneri della Toscana* **11**, 11–14. (in Italian).

Todini, E. 2003 A more realistic approach to the "extended period simulation" of water distribution networks. In *Advances in Water Supply Management* (ed. C. Maksimovic, D. Butler & F. A. Memon), pp. 173–184. A.A. Balkema Publishers, Lisse, The Netherlands.

Todini, E. & Pilati, S. 1988 A gradient method for the solution of looped pipe networks. In *Computer Applications in Water Supply* (ed. B. Coulbeck & C. H. Orr), Vol. 1, (System analysis and simulation) pp. 1–20. John Wiley & Sons, London.

Todini, E., Tryby, M. E., Wu, Z. Y. & Walski, T. M. 2007 Direct computation of variable speed pumps for water distribution system analysis. In *Water Management Challenges in Global Change* (ed. B. Ulanicki, K. Vairavamoorthy, D. Butler, P. L. M. Bounds & F. A. Memon), pp. 411–418. Taylor & Francis, London.

Ulanicka, K., Ulanicki, B., Rance, J. P. & Coulbeck, B. 1998 Benchmarks for water networks modelling. In *Hydroinformatics 1998*, Rotterdam, pp. 1469–1476.

Van Zyl, J., Savic, D. A. & Walters, G. A. 2006 Explicit integration method for extended-period simulation of water distribution systems. *J. Hydraulic Eng.* **132** (4), 385–392.

Water Research Centre 1994 *Analysis, Simulation and Costing of Water Networks and a Guide to the WATNET5.4 Computer Program*. Water Research Centre, Swindon, UK.

Wood, D. 1980 *Computer Analysis of Flow in Pipe Networks Including Extended Period Simulations*. User's manual, Univ. of Kentucky, Lexington, Ky.

Wood, D. J. & Charles, C. O. A. 1972 Hydraulic network analysis using linear theory. *J. Hydraulics Div.* **98**, Proc. Paper 9031, 1157–1170.

Wu, Z. Y., Tryby, M., Todini, E. & Walski, T. M. 2009 Modeling variable-speed pump operations for target hydraulic characteristics. *J. AWWA* **101** (1), 54–64.

First received 13 August 2009; accepted in revised form 11 November 2009. Available online 13 April 2010

APPENDIX: MODIFICATIONS REQUIRED TO RUN THE EXAMPLE WITH EPANET 2

The schematic network used in the example is composed of two tank nodes (1 and 2) and a reservoir node (3), and cannot be run using EPANET 2 which requires at least one junction node in the network. Therefore, as shown in Figure A1, an additional junction node 4 with null demand was added to the original scheme and connected to Tank n. 1 through a closed pipe n. 4. This inclusion does not modify the hydraulic behaviour of the system and can be run using EPANET 2.

For a better understanding of the schematization, the essential part of the EPANET 2 input file relevant to the description of the system is also given in Table A1.

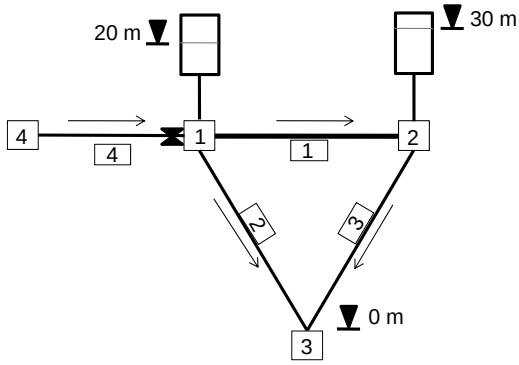

Figure A1 | Schematic representation of the example to be run using EPANET 2. A null demand junction node 4 and a closed pipe 4 were added to the original scheme without modifying the expected system behaviour.

Table A1 | A subset of the EPANET 2 input file with the description of the problem

```
[JUNCTIONS]
;ID Elev Demand Pattern
  4 0 0 ;

[RESERVOIRS]
;ID Head Pattern
  3 0 ;

[TANKS]
;ID Elevation InitLevel MinLevel MaxLevel Diameter MinVol VolCurve
  1 0 20 0 50 3.56 0 ;
  2 0 30 0 50 3.56 0 ;

[PIPES]
;ID Node1 Node2 Length Diameter Roughness MinorLoss Status
  1 1 2 100 200 130 0 Open ;
  2 1 3 100 100 130 0 Open ;
  3 2 3 100 100 130 0 Open ;
  4 4 1 100 100 130    0 Closed ;
```